

Article

Pd-Ag-Au Minerals in Clinopyroxenites of the Kachkanar Ural–Alaskan-Type Complex (Middle Urals, Russia)

Sergey Yu. Stepanov ¹, Ivan F. Chayka ^{2,*} , Roman S. Palamarchuk ¹ and Andrey V. Korneev ³

¹ Zavaritsky Institute of Geology and Geochemistry, Ural Branch of the Russian Academy of Sciences, 15 Akademika Vonsovskogo Str., 620016 Ekaterinburg, Russia; stepanov-1@yandex.ru (S.Y.S.)

² Korzhinsky Institute of Experimental Mineralogy, Russian Academy of Sciences, 4 Akademika Osipyana Str., 142432 Chernogolovka, Russia

³ South Urals Research Center of Mineralogy and Geoecology, Ural Branch of the Russian Academy of Sciences, Ilmensky Zapovednik, 456317 Miass, Russia

* Correspondence: ivanlab211@gmail.com

Abstract: The study of noble metal minerals of the Ural–Alaskan-type (UA-type) complexes has been traditionally focused on their platinum-bearing dunites and chromitites, while clinopyroxenites have been poorly considered. In this study, we report the first detailed data on the noble metal mineral assemblage in clinopyroxenites of the Kachkanar intrusion, which is a part of a UA-type complex and is renowned for its huge Ti-magnetite deposits. High concentrations of Pd, Au and Ag are closely linked to Cu-sulfide mineralization in amphibole clinopyroxenites, in which they form Pd-Ag-Au minerals: keithconnite Pd_{3–x}Te, sopcheite Ag₄Pd₃Te₄, stutzite Ag_{5–x}Te₃, hessite Ag₂Te, merenskyite PdTe, kotulskite Pd(Te,Bi), temagamite Pd₃HgTe, atheneite (Pd,Hg)₃As, potarite PdHg, electrum AuAg and Hg-bearing native silver. Among those, six mineral phases are first reported for clinopyroxenites of the Ural platinum belt. Our evidence supports a petrological model, suggesting that during fractionation of high-Ca primitive magmas at high oxygen fugacity, Pt, Os, Ir, Ru and Rh accumulate in early olivine–chromite cumulates, while Pd, Au and Ag reside in the melt until sulfide saturation occurs and then concentrate in sulfide mineralization. Subsequently, this sulfide mineralization is likely affected by cumulate degassing, which results in a partial resorption of the sulfides and Pd, Au and Ag remobilization by fluid. Second-stage concentration of the sulfides and the chalcophile noble metals in the amphibole-rich rocks may occur when H₂O from the fluid reacts with pyroxenes to form amphiboles, and the fluid becomes oversaturated with sulfides and chalcophile elements.

Keywords: Kachkanar intrusion; Ural–Alaskan-type complex; gold; palladium; copper; silver; Ural platinum belt; Russia



Citation: Stepanov, S.Y.; Chayka, I.F.; Palamarchuk, R.S.; Korneev, A.V. Pd-Ag-Au Minerals in Clinopyroxenites of the Kachkanar Ural–Alaskan-Type Complex (Middle Urals, Russia). *Minerals* **2023**, *13*, 1528. <https://doi.org/10.3390/min13121528>

Academic Editors: Basilios Tsikouras, Federica Zaccarini and Elena Ifandi

Received: 16 November 2023

Revised: 28 November 2023

Accepted: 29 November 2023

Published: 8 December 2023



Copyright: © 2023 by the authors. Licensee MDPI, Basel, Switzerland. This article is an open access article distributed under the terms and conditions of the Creative Commons Attribution (CC BY) license (<https://creativecommons.org/licenses/by/4.0/>).

1. Introduction

Clinopyroxenite is an ultramafic rock, composed of dominant (>50%) clinopyroxene, and may contain subordinate (<50% in total) hornblende and olivine and minor (<10%) plagioclase. Based on abundances of olivine and amphibole, olivine clinopyroxenites (>10% olivine) and amphibole clinopyroxenites (>10% amphibole) are distinguished [1]. Clinopyroxenites containing up to 10%–20% of magnetite are referred to as “magnetite clinopyroxenites”. Igneous clinopyroxenites are typical of the island arc high-Ca, high-Mg moderately alkaline (ankaramitic) magmatism. Olivine and magnetite clinopyroxenites are largely thought to form via magmatic differentiation of a melt saturated with clinopyroxene ± olivine ± magnetite. Hornblende (or other amphibole) presence is commonly attributed to water-saturated conditions of their crystallization or to postcumulus late-magmatic processes. The fact that relatively low Al₂O₃ content in the parental melt and elevated pressures are necessary to produce significant volumes of clinopyroxenitic cumulates explains the relative scarcity of these rocks among mafic–ultramafic cumulates [2,3]. The most

typical occurrences of igneous clinopyroxenites are Ural–Alaskan-type (UA-type) complexes, which are zoned intrusions, composed by dunites, clinopyroxenites (or wehrlites) and gabbros. Dunites of these complexes are typically populated by chromitite veins and schlieren, that may contain rich Pt mineralization, while gabbros commonly host hornblendite segregations [2,4]. The UA-type complexes have to a various extent a pronounced zoned structure. In undeformed and slightly deformed complexes, dunites occupy core parts and are surrounded by zones of clinopyroxenites and gabbros [5].

A series of Paleozoic mafic–ultramafic intrusions of the Ural platinum belt (UPB) can be divided into the Ural–Alaskan-type concentric dunite–clinopyroxenite–gabbro intrusions and those which are mainly composed of gabbro [6]. Noble-metal ores of the UA-type dunites and associated chromitites have been attracting much attention and have been studied in detail [7–18]. Considerable attention has been also paid to ore resources of the gabbros, as they contain copper deposits (e.g., large Volkovskoe deposit–Volkovsky complex) [19–21] and Pd–Cu ores (the Serebryanskiy Kamen’ massif, the Kumba intrusion) [22,23]. At the same time, much less is known about noble metal geochemistry and mineralogy in the clinopyroxenites, which are essential parts of the UA-type complexes of the UPB. Moreover, from a petrological perspective, olivine clinopyroxenites are suggested to form during cotectic olivine + clinopyroxene ± magnetite crystallization, which, along with the preceding chromite–olivine cotectic, represents a main stage of the differentiation of high-Ca, high-Mg (ankaramitic) magmas, which are supposed to be parental for the UA-type complexes [24–27]. Therefore, even though clinopyroxenites are not known to contain economic amounts of the noble metals and Cu, it is still essential to study their ore mineralization to improve our understanding of the ore-forming metals’ behavior during the magmatic stage of the UA-type complexes formation.

Thus far, elevated concentrations of Pd and Pt in clinopyroxenites have been reported for some intrusions of the UPB [28–30]. However, mineral phases hosting these elements have not yet been characterized sufficiently. Described in the most detail is the noble metal assemblage of the olivine clinopyroxenites from the Baronskoe–Kluevsky ore deposit (the Volkovsky complex) [29,30]. Several minerals of the noble metals have been previously identified in clinopyroxenites of the Kachkanar intrusion [28], but their occurrence and assemblages have not received attention. Finally, individual grains of stibiopalladinite Pd₅Sb₂ have been recently reported for phlogopite clinopyroxenites and hornblende peridotites of the Svetloborsky massif dykes [18].

In this study, aimed to partially fill the aforementioned gap, we report detailed data on noble metal mineralization in clinopyroxenites of the Kachkanar intrusion (a part of the Kachkanar UA-type complex), which belongs to the UPB and is renowned for both platinum-group element (PGE) placers and huge Ti-magnetite deposits [13,15,31–33]. We compare the noble metal mineralogy and geochemistry of this occurrence with the previously reported data on clinopyroxenites and dunites of the UPB. Given that the clinopyroxenites are important and essential intermediate members in the sequence from dunites to gabbros, characteristic of the UA-type complexes, this case study provides further insights into the behavior of the ore-forming metals during fractionation of the parental high-Mg, high-Ca arc magmas and formation of the UA-type complexes in general.

2. Geological Background

The Ural platinum belt is a large regional structure of the Ural fold belt. This belt is located at the western part of the Tagil megazone and comprises several igneous formations, among which a series of UA-type zoned complexes is distinguished (Figure 1a,b). These complexes are supposed to represent deep parts of the supra-subduction volcanic systems and are composed of a series of rocks ranging from dunites through to wehrlites and clinopyroxenites to gabbro and hornblendites [6,34–37]. At the modern erosional level, most of these complexes are dominated by either dunites or gabbros, while clinopyroxenites are subordinate. At the Kachkanar intrusion, however, clinopyroxenites are represented at a considerable area and are cropped out by open-pit mines, making this case a good

example to study them (Figure 1c,d). This intrusion is neighbored by the Svetloborsky and Veresovoborsky clinopyroxenite–dunite intrusions (westwards) and by the Mt. Sarannaya gabbroic intrusion (northwards) (Figure 1c). As suggested by [13,36] and the State Geological Map [36], these four intrusions: Kachkanar, Svetloborsky, Veresovoborsky and Mt. Sarannaya—compose a single UA-type complex. Following the classification of [37], hereinafter in the text we refer to the studied clinopyroxenite-dominated body as the Kachkanar intrusion, while the UA-type assemblage, consisting of these four intrusions, is addressed as the Kachkanar complex.

The Kachkanar intrusion penetrates Ordovician metavolcanics of the Mariinsky formation (one of the main formations of the West-Tagil megazone), which are composed by greenschist-metamorphosed aphyric and, more occasionally, porphyric basalts [37]. The intrusion has a total area of ~111 km² and is composed of two clinopyroxenitic bodies largely surrounded by olivine gabbros (Figure 1c). The open-pit mines of the Kachkanar Ti-Fe deposit (Figure 1d) crop out one of these bodies, which has a longitudinally elongated shape of about 8.5 km long and steeply dipping eastwards [38]. The rocks, cropped out by the pit, are composed of dominant clinopyroxenites, minor amphibole clinopyroxenites, olivinites (chromite-free olivine–magnetite rocks), wehrlites, hornblendites and vein rocks. Among clinopyroxenites, the most typical are magnetite olivine-free and plagioclase-free varieties. These rocks contain economic Ti-Fe ores (15%–20% FeO, ~2% TiO₂ in oxide form), which occur as medium-grade to rich disseminated, vein-disseminated or banded textures formed by titanomagnetite aggregations. These magnetite clinopyroxenites host enclave- or dyke-like bodies of amphibole clinopyroxenites, one of which was the object of our study (Figure 2).

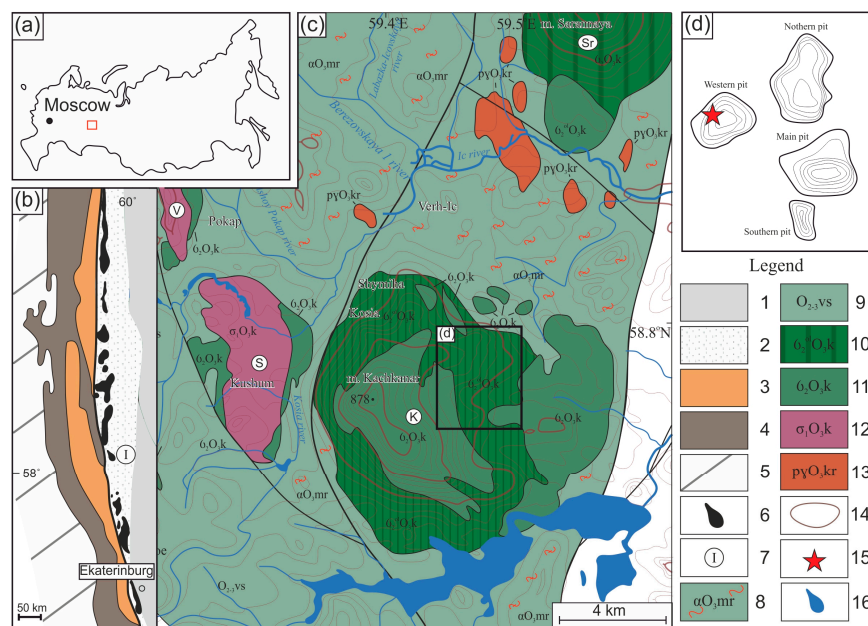


Figure 1. Location of the Kachkanar intrusion and its geological features. (a) = Position on the map of Russia; (b) = location of the UPB in a general structure of the Ural orogenic belt (after [39]); (c) = Geological map of the Kachkanar intrusion (K) and the surrounding Veresovoborsky (V), Svetloborsky (S) and Mt. Sarannaya (Sr) intrusions (after [37]). (d) = schematic sketch of the open-pit mines of the eastern part of the Kachkanar intrusion. Legend: 1 = East Ural megazone; 2 = Tagil megazone, 3 = Central Ural megazone, 4 = West Ural megazone, 5 = Eastern Europe platform, 6 = mafic–ultramafic complexes of the UPB; 7 = location of the Kachkanar intrusion; 8 = metavolcanics of the Mariinsky formation; (9) = volcano-sedimentary rocks of the Viyskaya formation, (10–12) = rocks of the Kachkanar complex: olivine gabbros (10), clinopyroxenites (11) and dunites (12); (13) = plagiogranites of the Krivinsky complex; (14) = contour lines (isohypses); (15) = sampling location, (16) = water reservoirs.

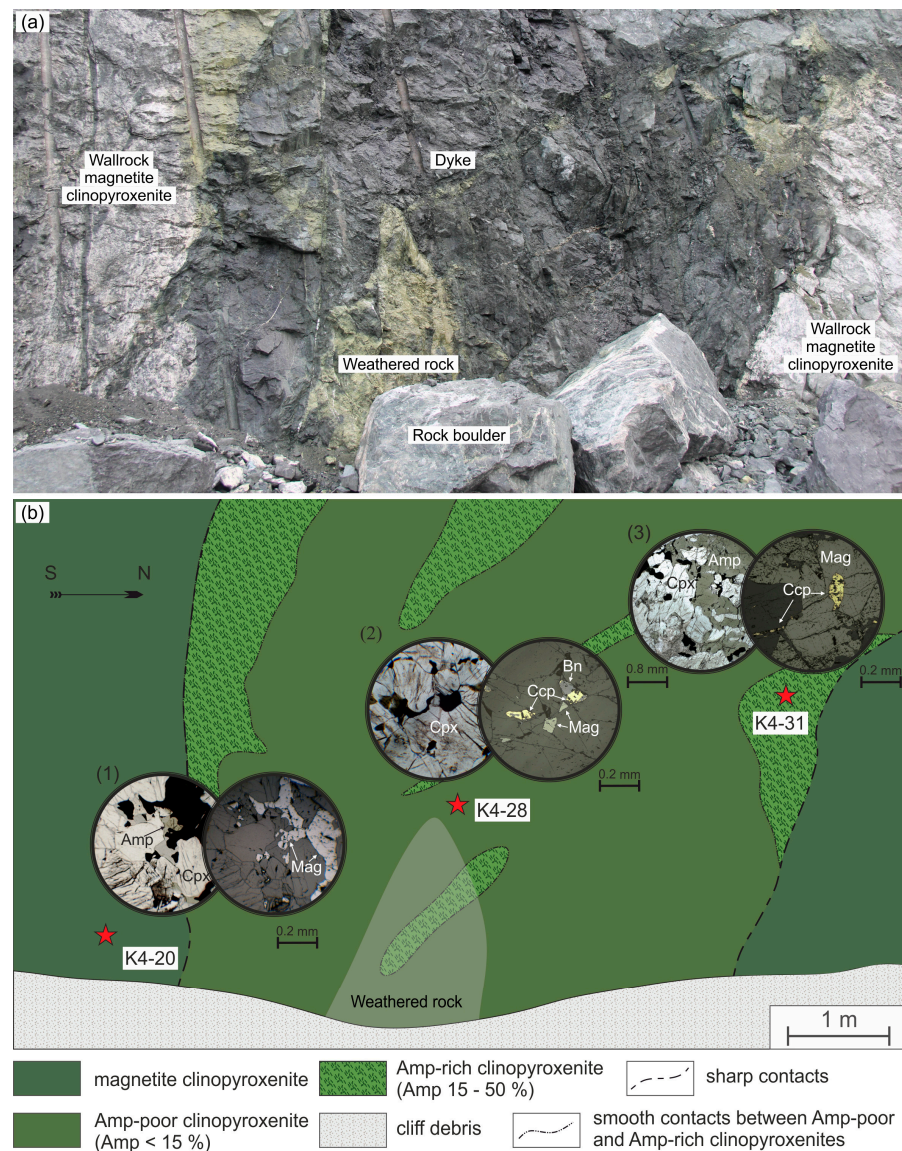


Figure 2. A photograph of the sampling site at the Western mine of the deposit (a) and its schematic sketch with the sample locations and optical photomicrographs of the samples (b). Rock varieties: K4-20—magnetite clinopyroxenite; K4-28—dyke amphibole-poor clinopyroxenite; K4-31—dyke amphibole-rich (amphibole) clinopyroxenite.

3. Samples and Methods

3.1. Samples

At the Western open-pit mine of the deposit, coarse-grained magnetite ore clinopyroxenites are penetrated by a 6–7 m thick dyke (Figure 2a) of medium-to-fine-grained clinopyroxenites with less magnetite, but containing significant sulfides (5–7 vol. % on average). The host clinopyroxenites are rich in interstitial and sideronitic magnetite, which forms vein texture. The dyke is characterized by lithological heterogeneity manifested in the patchy distribution of subordinate amphibole. Macroscopically, amphibole-rich clinopyroxenites are composed of diopside (~60%), amphibole (20%) and secondary and ore minerals (20%). In the axial part and contact zones of the dyke, there are segregations containing 60 vol. % and more amphibole: up to monomineralic hornblendites (Figure 2b).

Hand specimens (0.5–1.5 kg) (Table 1) and high-weight panel samples (24 kg on average) were collected from the host magnetite clinopyroxenites and the dyke. Polished sections and thin sections were made from the hand samples. Heavy concentrates have

been extracted from the panel samples by crushing them to <1 mm fraction with subsequent gravitational concentration.

Table 1. A list of the main studied samples and their brief characteristics.

Sample No.	Rock Type	Cpx	Amp	Mag	Sulf
K4-20	Host rock magnetite clinopyroxenite	47	<1	50	1
K4-22	Host rock magnetite clinopyroxenite	81	3	15	<1
K4-23	Host rock magnetite clinopyroxenite	80	<1	18	1
K4-21	Dyke amphibole-poor clinopyroxenite	70	7	22	<1
K4-28	Dyke amphibole-poor clinopyroxenite	80	5	12	3
K4-30	Dyke amphibole clinopyroxenite	55	30	10	5
K4-31	Dyke amphibole clinopyroxenite	40	43	10	7

Mineral abbreviations: Cpx = clinopyroxene, Amp = amphibole, Mag = magnetite, Sulf = sulfide. Contents of the minerals are given in vol. % estimated based on their area proportions in a thin section.

3.2. Analytical Methods

Preliminary examination of the samples with identification of the main silicate, accessory and ore minerals and their structural relationships has been carried out using optical microscopy (transmitted and reflected plane- and cross-polarized light).

The chemical composition of the minerals has been analyzed using (1) scanning electron microscope JEOL JSM-6390LV equipped with an X-ray energy dispersion spectrometer and (2) electron microprobe with an X-ray wavelength dispersion spectrometer Camebax SX100 (Center for Collective Research “Geoanalitik”, Institute of Geology and Geochemistry Uralian Branch of the Russian Academy of Sciences—IGG UB RAS, Yekaterinburg, Russia).

Bulk rock contents of the PGEs and Au were determined by fire assay method on nickel matte with ICP-MS ending using an XSeries2 mass spectrometer (Laboratory of the Gipronickel Institute LLC, Saint Petersburg; state certificates STP 35-12-241 and STP 35-12-282) with detection limits (ppb): Os—10, Ir—3, Ru—5, Rh—5, Pt—10, Pd—5, Au—10.

4. Results

4.1. Petrographical Features of the Rocks

Magnetite clinopyroxenites of the host rock (samples K4-20, K4-22, K4-23) are dominated (~70 vol. %) by clinopyroxene. Clinopyroxene (diopside) forms isometric (with nearly equal dimensions), colorless grains with an average size of 3.2 mm. Less than 10 vol. % of the clinopyroxenites is formed by dark-green amphibole, the abundance of which is higher in fine-grained aggregations of clinopyroxene and magnetite and lower in the other textural varieties of these rocks. Magnetite (15–25 vol. %) forms anhedral grains and interstitial and sideronitic aggregations within the silicate matrix (Figure 3a). In certain samples, magnetite abundance reaches 40 vol. % and more (Table 1), forming schlieren and dense dissemination. The mineral composition of these clinopyroxenites is generally the same as that of the other magnetite clinopyroxenites of the Kachkanar complex and the UPB in general.

Medium-to-fine-grained amphibole-poor clinopyroxenites (samples K4-21, K4-28), which form the major part of the dyke, are texturally homogeneous. About 80–90 vol. % of the rock is made of clinopyroxene, which forms euhedral and subhedral prismatic or tabular crystals with an average size of 1.2 mm. Tiny grains of amphibole occur in interstices between clinopyroxene and magnetite grains (Figure 3b). Ore minerals are dominated by magnetite (~10 vol. %), although sulfides (chalcopyrite and bornite) typically occur (1–3 vol. %) as well. Mineralogical features of these clinopyroxenites are similar to those of the magnetite clinopyroxenites, which host the dyke, yet magnetite is generally less abundant in the dyke clinopyroxenites.

Amphibole clinopyroxenites (samples K4-30, K4-31), which form patches in the clinopyroxenitic dyke, contain 45%–60% clinopyroxene (diopside), 30%–45% amphibole (pargasite–magnesiostastingsite) and 10%–20% of ore (magnetite, sulfides) and secondary minerals. The main rock-forming silicates are subhedral and make up a prismatic

grained fine- and medium-grained texture of the rock (Figure 3c). Not uncommon is the overgrowth of clinopyroxene grains by amphibole, which forms coronitic structures.

A typical secondary mineral in these rocks is actinolite, which acicular and fibrous crystals form sheaf-like aggregations that replace primary clinopyroxenes. Less abundant is acicular actinolite–tremolite, which replaces large crystals of magnesiohastingsite. This kind of replacement implies that the studied rocks have been slightly metamorphosed in conditions of a greenschist facies.

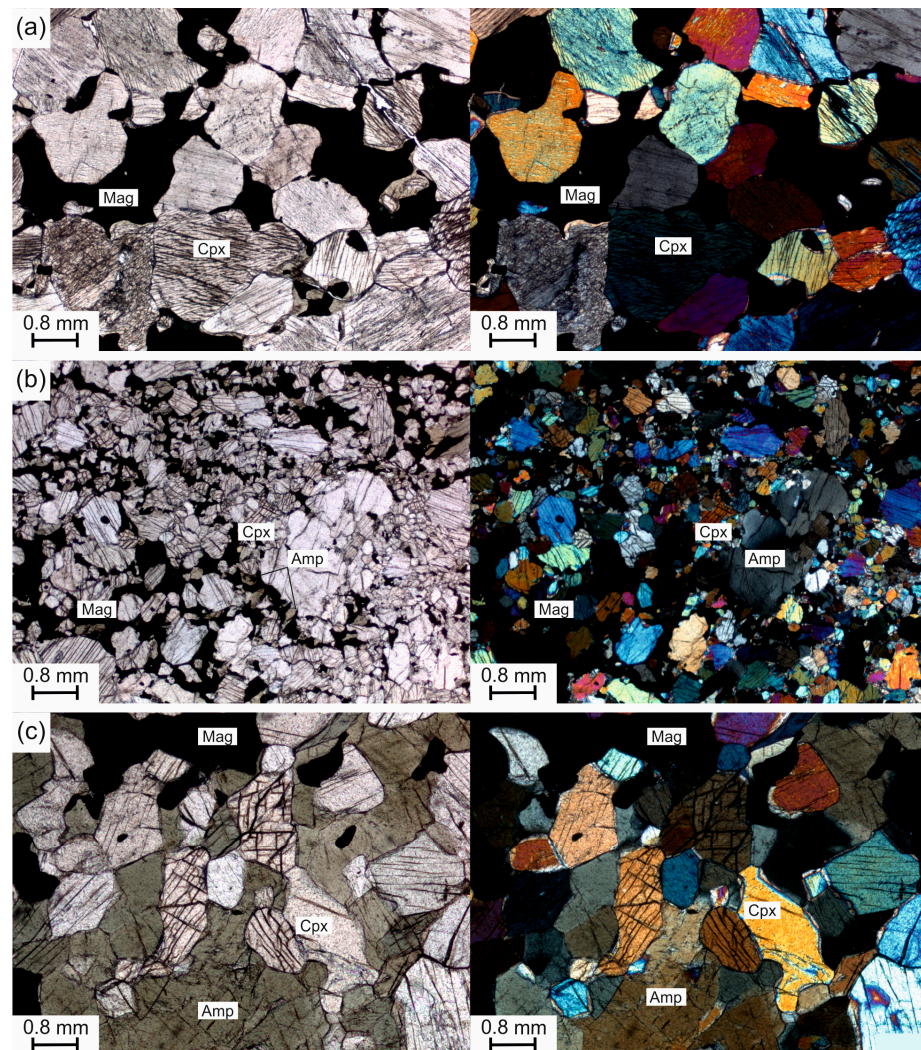


Figure 3. Transmitted light photomicrographs of the representative thin section of the studied rocks. (a) = magnetite clinopyroxenite, (b) = amphibole-poor clinopyroxenite from the dyke; (c) = amphibole clinopyroxenite from the dyke. (Left) parts of the panels—plane-polarized light; (right) ones—cross-polarized light. Mineral abbreviations are given according to [40]: Mag = magnetite, Cpx = clinopyroxene, Amp = amphibole (pargasite–magnesiohastingsite).

4.2. Composition of the Rock-Forming Minerals

Clinopyroxene is the main rock-forming mineral in the studied rocks. Clinopyroxene from the magnetite clinopyroxenites is diopside with Al_2O_3 content varying around 2.2–2.7 wt.% and TiO_2 from 0.2 to 0.26 wt.%. Clinopyroxene from amphibole clinopyroxenites is diopside and augite with high Al_2O_3 (3.5–6.4 wt.%) and elevated TiO_2 (0.54–1.05 wt.%) concentrations. Cr_2O_3 in all clinopyroxenes analyzed is below 0.05 wt.% and Na_2O varies from 0.1 to 0.2 wt.% (Table 2).

Table 2. Representative EPMA analyses of clinopyroxene from the studied rocks (wt.%).

Components	K4-30	K4-30	K4-31	K4-31	K4-20	K4-20	K4-20	K4-20
SiO ₂	47.65	48.8	51.04	51.14	52.01	52.18	52.02	52.37
MgO	12.99	13.41	14.22	14.3	15.37	15.88	16.03	15.26
CaO	24.63	25.04	24.13	24.06	23.99	24.27	23.96	23.94
Cr ₂ O ₃	bdl	bdl	0.04	bdl	0.05	bdl	0.03	0.02
FeO	6.91	5.55	6.31	6.57	5.51	4.69	4.79	5.23
MnO	0.15	0.13	0.22	0.28	0.12	0.13	0.12	0.15
NiO	bdl	0.02	bdl	bdl	0.02	bdl	0.04	0.03
Al ₂ O ₃	6.38	6.02	3.74	3.49	2.63	2.51	2.56	2.62
Na ₂ O	0.16	0.1	0.25	0.15	0.19	0.15	0.13	0.17
K ₂ O	0.03	0.02	0.06	0.02	bdl	bdl	Bdl	Bdl
TiO ₂	0.83	1.05	0.57	0.54	0.23	0.22	0.21	0.28
Total	99.73	100.14	100.58	100.55	100.12	100.03	99.90	100.07
Atoms per formula unit calculated on the basis of 6 oxygen atoms								
Si	1.791	1.813	1.886	1.891	1.919	1.921	1.918	1.929
Mg	0.728	0.743	0.783	0.788	0.845	0.871	0.881	0.838
Ca	0.992	0.997	0.955	0.953	0.948	0.957	0.946	0.945
Cr	-	-	0.001	0.000	0.001	-	0.001	0.001
Fe	0.217	0.172	0.195	0.203	0.170	0.144	0.148	0.161
Mn	0.005	0.004	0.007	0.009	0.004	0.004	0.004	0.005
Ni	-	0.001	-	-	0.001	-	0.001	0.001
Al	0.283	0.264	0.163	0.152	0.114	0.109	0.111	0.114
Na	0.012	0.007	0.018	0.011	0.014	0.011	0.009	0.012
K	0.001	0.001	0.003	0.001	-	-	-	-
Ti	0.023	0.029	0.016	0.015	0.006	0.006	0.006	0.008

bdl: below the detection limit.

Amphibole is represented by several generations, which were apparently formed due to different processes. The first generation (magmatic) is moderately Ti pargasite and magnesiohastingsite, which forms its own grains in the interstices between clinopyroxene crystals or corona structures around clinopyroxene. More occasional are large poikilitic grains of pargasite, which host smaller grains of diopside. This amphibole is compositionally homogeneous in all samples studied and contains 2.0–2.3 wt.% Na₂O, a significant (up to 0.9%) admixture of K₂O and 1.0–1.7 wt.% TiO₂ (Table 3). The second generation (post-magmatic, metamorphic) is represented by fibrous and acicular amphiboles, replacing primary silicates. They are of the actinolite–tremolite series and, more occasionally, are represented by ferrohornblende.

Table 3. Representative EPMA analyses of amphibole from the studied rocks (wt.%).

	K4-30	K4-30	K4-31	K4-31	K4-20	K4-20	K4-20	K4-20
SiO ₂	40.55	40.64	40.99	40.45	40.46	39.99	40.48	41.03
TiO ₂	1.14	1.22	1.03	1.31	1.56	1.57	1.66	1.61
Al ₂ O ₃	15.76	15.05	15.03	14.89	14.55	14.49	14.42	14.85
FeO	9.33	8.63	9.52	9.71	9.93	10.20	9.81	8.66
MgO	14.18	14.32	14.28	14.12	14.21	13.96	14.05	14.69
MnO	0.17	0.03	0.08	0.04	0.07	0.11	0.11	0.11
CaO	13.1	12.97	12.97	12.98	12.91	12.91	12.84	13.08
Na ₂ O	2.26	2.31	2.22	2.2	2.02	2.09	2.00	2.12
K ₂ O	0.78	0.86	0.79	0.77	0.87	0.86	0.82	0.55
Total	97.29	96.03	96.91	96.47	96.60	96.19	96.19	96.70
Atoms per formula unit calculated on the basis of 6 oxygen atoms								
Si	5.959	6.031	6.045	6.005	6.007	5.980	6.030	6.034
Ti	0.126	0.136	0.114	0.146	0.174	0.177	0.186	0.178
Al	2.730	2.632	2.612	2.605	2.546	2.554	2.531	2.574
Al ^{IV}	2.041	1.969	1.955	1.995	1.993	2.020	1.970	1.966
Al ^{VI}	0.689	0.663	0.657	0.610	0.554	0.534	0.561	0.608

Table 3. Cont.

	K4-30	K4-30	K4-31	K4-31	K4-20	K4-20	K4-20	K4-20
Fe	1.147	1.071	1.174	1.206	1.233	1.276	1.222	1.065
Mg	3.106	3.168	3.139	3.125	3.145	3.112	3.120	3.221
Mn	0.021	0.004	0.010	0.005	0.009	0.014	0.014	0.014
Ca	2.063	2.062	2.049	2.065	2.054	2.068	2.049	2.061
Na	0.644	0.665	0.635	0.633	0.582	0.606	0.578	0.604
K	0.146	0.163	0.149	0.146	0.165	0.164	0.156	0.103

4.3. Fe-Ti Oxide and Base Metal Sulfide Mineralization

Ore mineralization in the studied varieties of clinopyroxenites has a relatively uniform mineral composition. Compositional and structural features of Ti-magnetite ores have been extensively studied [38]. Here, we only briefly describe Fe-Ti oxide mineralization and focus more on base metal sulfide and noble metal (see Section 4.4) mineralization.

The main ore mineral in the clinopyroxenites is magnetite, which content varies from the ~1% to tens of per cent. The most typical are large (up to 4–5 mm) interstitial anhedral grains and aggregations of magnetite, which contain lamellar and lattice-like exsolutions of spinel-group minerals (mainly ulvöspinel) (Figure 4a,b). Ilmenite is the second abundant ore mineral in the magnetite clinopyroxenites. Two morphological varieties are characteristic of ilmenite. The first variety is represented by large platy and tabular crystals intergrown with anhedral magnetite (Figure 4c). The second variety is represented by thin exsolution lamellae in magnetite. Sulfide mineralization is scarce and is represented by bornite–chalcopyrite aggregates included within magnetite.

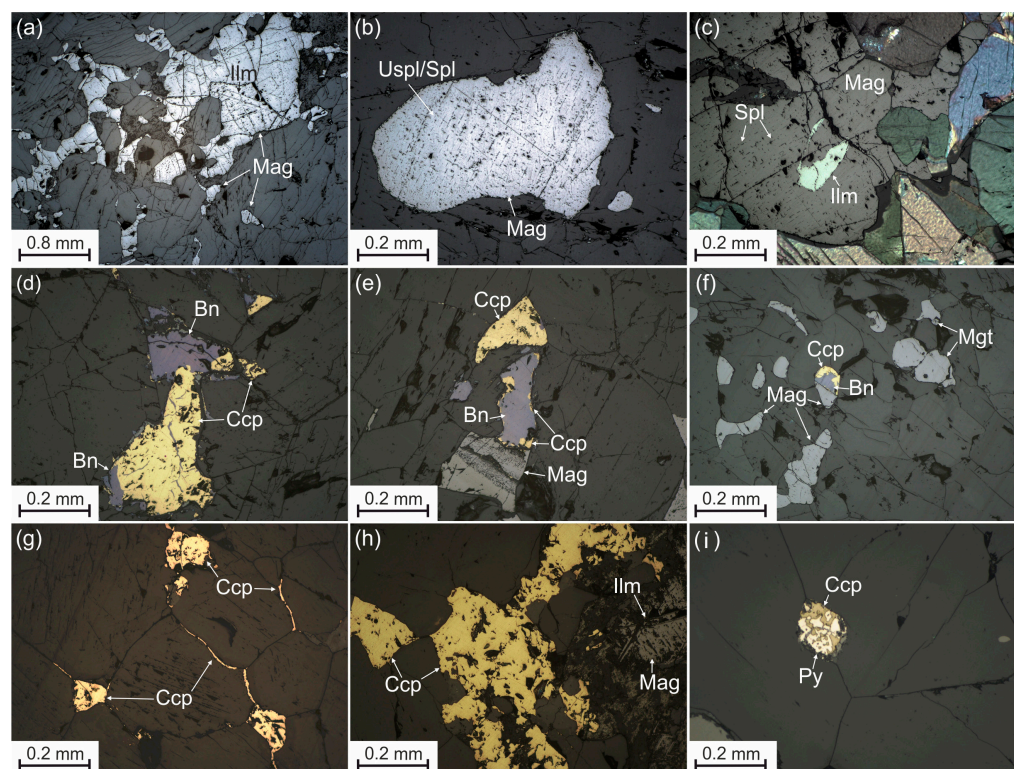


Figure 4. Reflected light photomicrographs of the ore mineral assemblages. (a–c) = Ti-magnetite assemblage in the magnetite clinopyroxenites; photo at (c) is in semi-crossed polarized light to highlight anisotropic ilmenite within an isotropic magnetite; (d–f) = chalcopyrite–bornite–magnetite assemblage in the dyke amphibole-poor clinopyroxenites; (g–i) = pyrite–chalcopyrite assemblage in the dyke amphibole clinopyroxenites. Mineral abbreviations are given according to [39]: Bn = bornite, Ccp = chalcopyrite, Ilm = ilmenite, Mag = magnetite, Spl = spinel, Py = pyrite, Uspl = ulvöspinel.

Considerable sulfide mineralization is hosted by the fine- and medium-grained amphibole-rich clinopyroxenites, composing the dyke. Sulfides in these rocks are located in interstices between clinopyroxene and, occasionally, pargasite crystals. Sometimes, sulfides are intergrown with magnetite. Based on structural relationships between the ore minerals in the clinopyroxenites, we distinguish two main ore assemblages, which have contrasting compositional, structural and textural features.

The first is the chalcopyrite–bornite–magnetite assemblage, occurring both in amphibole-poor and amphibole clinopyroxenites from the dyke. The most abundant of this type is magnetite, which is similar to that from the magnetite clinopyroxenites (Figure 4d–f). Sulfides are largely represented by chalcopyrite and bornite. Magnetite and sulfides largely form intergrowths with an intricate boundary between the phases (Figure 4e,f). Replacement of bornite and chalcopyrite by chalcocite and covellite is most manifested along fractures and boundaries of the chalcopyrite–bornite aggregations. The size of grains and aggregations of bornite and chalcopyrite varies mainly in the range of 0.1–1.3 mm with an average value of ~0.6 mm. The texture of the base metal sulfide (BMS) mineralization is disseminated, interstitial up to sideronitic in the richest varieties.

The second type of assemblage (pyrite–chalcopyrite) is particularly characteristic of the amphibole clinopyroxenites from the dyke. The dominant sulfide in this type is chalcopyrite, which forms granular aggregations with the grain size reaching several mm. The aggregations are mainly located in interstices between silicates and magnetite. Common are thin chalcopyrite stringers, following margins between rock-forming silicates (Figure 4g). Occasionally, there are chalcopyrite veins (Figure 4h) up to several mm thick, along which rock-forming silicates and magnetite are replaced by chlorite and actinolite. Intricate intergrowths of pyrite and chalcopyrite are subordinate and do not exceed 0.2 mm (Figure 4i).

Compositions of the gravitational concentrates extracted from the dyke clinopyroxenites and the wall-rock magnetite clinopyroxenites support the in situ observations. The concentrate extracted from the magnetite clinopyroxenites is dominated by magnetite, ilmenite and silicate minerals (mainly clinopyroxene). Minor are the sulfides: pyrite, chalcopyrite and pyrrhotite (Figure 5a). The concentrates extracted from the dyke rocks (both amphibole-poor and amphibole clinopyroxenites) are dominated by chalcopyrite and bornite. In addition to the in situ described sulfides, these concentrates contain pyrrhotite, carrolite CuCo_2S_4 and galena (Figure 5b).

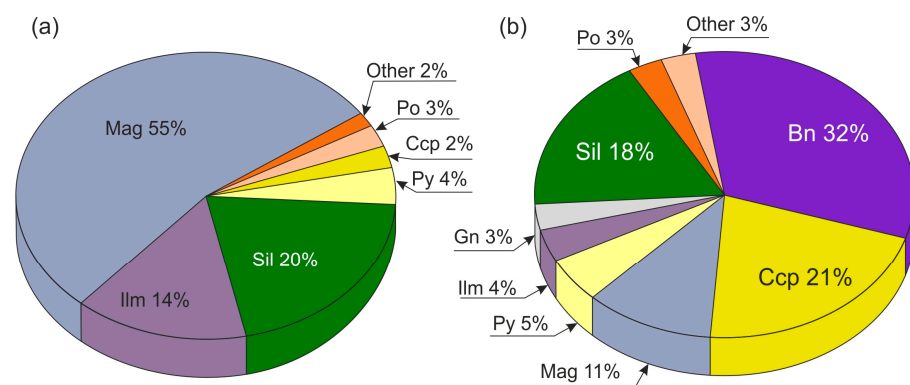


Figure 5. Pie charts reflecting phase proportions in the gravitational concentrates. (a) = of the magnetite clinopyroxenites, (b) = of the amphibole clinopyroxenites. Abbreviations: Bn—bornite, Ccp—chalcopyrite, Gn—galena, Ilm—ilmenite, Mag—magnetite, Sil—silicates (mainly clinopyroxene), Py—pyrite, Po—pyrrhotite. Other—single grains of pentlandite and carrolite (CuCo_2S_4).

4.4. Pd-Au-Ag Mineralization

Both in situ mineralogical observations and the composition of the heavy concentrates show that the noble metal mineralization in all rocks considered is distinctly associated with Cu-sulfides. Most Pd, Au and Ag minerals were found in the amphibole clinopyroxenites

from the dyke (Table 4). Only certain micron-scaled occurrences of merenskiyite PdTe have been found intergrown with bornite and chalcopyrite from the wall-rock magnetite clinopyroxenites.

Table 4. Noble metal mineral abundances in clinopyroxenites and gabbros of the UPB and in dunites of the Svetloborsky and Veresovoborsky intrusions (genetically linked with the Kachkanar intrusion).

Mineral	Formula	Kachkanar Intrusion (This Study)	Kachkanar Intrusion [28]	Volkovsky Complex (Baronskoe-Kluevsky and Volkovskoe Ore Deposits) [29,30]	Svetloborsky and Veresovoborsky Dunite-Hosted Chromitites [14–18,41]	Serebryansky Kamen' and Kumba Gabbros [22,23]
ALLOYS AND INTERMETALLIDES						
Isoferroplatinum	Pt ₃ Fe	–	–	–	+++	–
Tetraferroplatinum	PtFe	–	✓	–	+++	–
Ferroan Platinum	Pt ₂ Fe	–	✓	–	++	–
Osmium	(Os,Ir,Ru)	–	–	–	++	–
Iridium	(Ir,Os,Ru)	–	–	–	++	–
Electrum	(Au,Ag)	++	–	+	–	–
Native silver	Ag	++	–	–	–	–
Native gold	Au	–	✓	+	–	++
Tulameenite	Pt ₂ CuFe	–	–	–	✓	–
Potarite	PdHg	++	✓	–	+	–
SULFIDES						
Laurite	RuS ₂	–	–	–	++	–
Erlichmanite	OsS ₂	–	–	–	✓	–
Cooperite	PtS	–	–	–	+	–
Vysotskite	(Pd,Ni)S	–	✓	+++	–	+++
Braggite	(Pt,Pd,Ni)S	–	✓	–	–	–
TELLURIDES						
Merenskiyite	PdTe	+	–	+++	–	+++
Hessite	Ag ₂ Te	++	–	++	–	++
Stutzite	Ag _{5–x} Te ₃	++	–	++	–	++
Kotulskite	Pd(Te,Bi) ₂	+++	✓	++	–	++
Sopcheite	Ag ₄ Pd ₃ Te ₄	++	–	–	–	–
Keithconnite	Pd _{3–x} Te	+	–	–	–	+
Michenerite	PdBiTe	–	–	–	–	+++
Atheneite	(Pd,Hg) ₃ As	++	✓	–	–	–
Temagamite	Pd ₃ HgTe ₃	+++	–	++	–	–
ARSENIDES AND ANTIMONIDES						
Mertieite	Pd ₅ (Sb,As) ₂	–	✓	–	–	++
Isomertieite	Pd ₁₁ Sb ₂ As ₂	–	✓	++	–	–
Stibiopalladinite	Pd ₅ Sb ₂	–	–	–	–	++
Arsenopalladinite	Pd ₈ (As,Sb) ₃	–	–	–	–	+
Stillwaterite	Pd ₈ As ₃	–	–	++	–	–
Vincentite	Pd ₃ As	–	–	–	–	+
Sperrylite	PtAs	–	–	–	–	+

Mineral abundances: +++ = dominant (>10% of all noble metal mineral findings), ++ = subordinate (1–10%), + = rare (<1%), ✓ = no data on abundance, “–” = absent. Host rocks for the mineralization: this study—amphibole clinopyroxenites from dyke; [28]—magnetite clinopyroxenites; [29,30]—sulfide-rich (>5% sulfides) clinopyroxenites of the Volkovsky complex.

Most of the noble metal mineral phases occur as small (<10 µm) grains or intergrowths, enclosed within bornite or bornite–chalcopyrite aggregates. Representative chemical microprobe analyses of the noble metal phases are listed in Table 5. In total, we identified 11 mineral species, including palladium and silver tellurides (keithconnite Pd_{3–x}Te, merenskiyite PdTe, stutzite Ag_{5–x}Te₃, sopcheite Ag₄Pd₃Te₄ and hessite Ag₂Te), Pd bismotellurides (kotulskite Pd(Te,Bi)), Pd-Hg chalcogenides (temagamite Pd₃HgTe, atheneite (Pd,Hg)₃As), potarite PdHg, electrum AuAg and Hg-bearing native silver (Table 4).

Kotulskite with an average formula Pd_{1.00}(Te_{0.73}Bi_{0.24}Hg_{0.02})_{0.99} predominates among minerals of the Pd-Te-Bi system. This mineral forms grains up to 50 µm in size, included within bornite (Figure 6a). In a gravitational concentrate, a single intergrowth of kotulskite

with an electrum $\text{Ag}_{0.55}\text{Au}_{0.33}\text{Cu}_{0.12}$ and sopcheite $\text{Ag}_{4.18}\text{Pd}_{2.90}\text{Au}_{0.10}\text{Te}_{3.82}$ has been found as a bornite-hosted isometric inclusion (Figure 6b). Importantly, there is an Au- and Ag-rich halo around the inclusion in the host bornite. Sopcheite forms either intergrowths with the other noble metal minerals or occurs as small (<20 μm) rounded inclusions within Cu-Fe sulfides (Figure 6c,d). Less common are merenskyite $\text{Pd}_{1.01}(\text{Te}_{2.01}\text{Bi}_{0.13})_{1.99}$ and keithconnite $\text{Pd}_{2.98}\text{Te}_{1.02}$, which typically occur as monomineralic inclusions in the Cu-Fe sulfides.

Table 5. Representative EDS chemical analyses of the noble metal minerals.

Components	Kt	Tem	Sop	Hes	Stz	Mrk	Ah	Kei	Ptr	Elc	Ag
Pd	41.82	34.96	24.38	–	–	28.95	55.89	70.91	33.96	–	–
Au	–	–	1.48	–	–	–	–	–	–	49.25	19.39
Ag	–	–	35.6	62.83	56.05	–	–	–	–	45.08	63.83
Cu	–	–	–	–	–	–	–	–	0.76	5.67	–
Te	36.66	42.5	38.54	37.17	43.95	63.88	–	29.09	–	–	–
Hg	1.74	22.54	–	–	–	–	23.58	–	65.28	–	16.78
Bi	19.78	–	–	–	–	7.17	–	–	–	–	–
As	–	–	–	–	–	–	20.53	–	–	–	–
Formula coefficients											
Pd	1.00	2.97	2.90	–	–	1.01	2.29	2.98	0.97	–	–
Au	–	–	0.10	–	–	–	–	–	–	0.33	0.13
Ag	–	–	4.18	2.00	4.81	–	–	–	–	0.55	0.76
Cu	–	–	–	–	–	–	–	–	0.04	0.12	–
Te	0.73	3.01	3.82	1.00	3.19	1.86	–	1.02	–	–	–
Hg	0.02	1.02	–	–	–	–	0.51	–	0.99	–	0.11
Bi	0.24	–	–	–	–	0.13	–	–	–	–	–
As	–	–	–	–	–	–	1.20	–	–	–	–

(Kt) kotulskite, (Tem) temagamite, (Sop) sopcheite, (Hes) hessite, (Stz) stutzite, (Mrk) merenskyite, (Ah) atheneite, (Kei) keithconnite, (Ptr) potarite, (Elc) electrum, (Ag) native silver $\text{Ag}_{0.76}\text{Au}_{0.13}\text{Hg}_{0.11}$. All compositions are normalized to 100%.

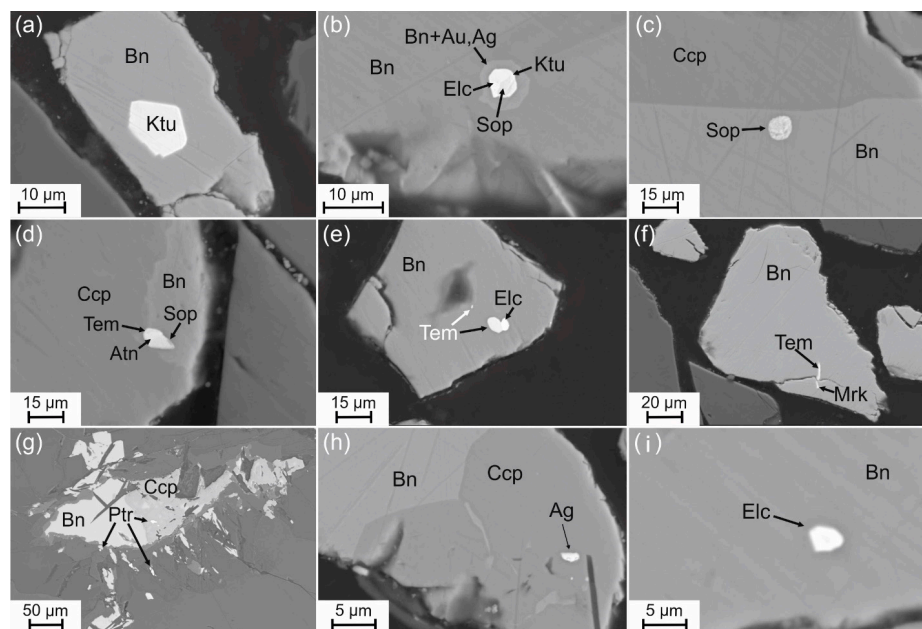


Figure 6. Backscattered electron photomicrographs of the noble metal minerals. (a) = a large crystal of kotulskite (Kt) in bornite (Bn) [18]; (b) = an intergrowth of electrum (Elc), kotulskite (Ktu) and sopcheite (Sop) in bornite surrounded by an aureole of Au- and Ag-bearing bornite (possibly due to a signal from an “appearing through” Au-Ag phase); (c) = rounded inclusion of sopcheite in bornite; (d) = an intergrowth of sopcheite, temagamite (Tem) and atheneite (Atn) in a bornite–chalcopyrite intergrowth; (e) = an intergrowth of temagamite and electrum [18]; (f) = a needle-like intergrowth of temagamite and merenskyite (Mrk) in a bornite grain; (g) = small inclusions of potarite (Ptr) scattered in a bornite–chalcopyrite intergrowth; (h) = silver native (Ag) in chalcopyrite; (i) = a small bornite-hosted inclusion of electrum. Mineral abbreviations are given according to [40].

Another group of platinum group minerals (PGMs) is represented by various Pd-Hg chalcogenides. The dominant one is temagamite, which, along with kotulskite, is a major noble metal mineral in the studied rocks. Temagamite occurs mostly as monomineralic grains, yet its intergrowths with electrum, sopcheite and ateneite $\text{Pd}_{1.89}\text{As}_{0.89}\text{Hg}_{0.38}$ (Figure 6d,e) are not uncommon. It has been noticed that being intergrown with electrum, temagamite contains up to 2.04% of Pt admixture. Finally, a single intergrowth of temagamite with merenskiyte has been found (Figure 6f). In addition to temagamite and atheneite, potarite $\text{Pd}_{0.97}\text{Cu}_{0.04}\text{Hg}_{0.99}$ has been found in situ in polished sections. Potarite (Figure 6g) occurs as fine (<10 μm) dispersed dissemination in bornite–chalcopyrite aggregates and largely contains admixtures of Cu (1.1 wt.% on average) and, occasionally, Au (up to 4.3 wt.%).

Quite common for the bornite–chalcopyrite aggregates are inclusions of gold and silver tellurides: hessite $\text{Ag}_{2.00}\text{Te}_{1.00}$ and stutzite $\text{Ag}_{4.81}\text{Te}_{3.19}$. The size of these phases does not exceed 20 μm , and they never form intergrowths with other noble metal minerals.

Gold and silver alloys are less common than the noble metal chalcogenides. They form small (generally <10 μm) isometric and rounded inclusions in bornite (Figure 6h,i). The content of Au in these phases varies from 40.3 to 58.5 wt.%. All alloys analyzed contain Cu and Hg impurities, which content reaches 7.53 and 2.75 wt.%, respectively. A single grain of silver native $\text{Ag}_{0.76}\text{Au}_{0.13}\text{Hg}_{0.11}$ has been found (Figure 6i). It is characterized by a heterogeneous distribution of Hg (8.1–16.8 wt.%) and Au (up to 30.0%) concentrations.

4.5. Noble Metal Geochemistry

To test the mineralogical data against the bulk rock geochemistry, bulk PGE + Au analyses have been performed on samples K4-20 (magnetite clinopyroxenite) and K4-30 (amphibole clinopyroxenite from the dyke). In addition, four bulk chemical compositions of these rock varieties have been borrowed from [28,42]. In our analyses, concentrations of Os, Ir, Ru and Rh were below the limits of detection (see Methods). Quantities of Pt, Pd and Au in magnetite clinopyroxenites are nearly equal and do not exceed 20 ppb, whilst amphibole clinopyroxenites contain more of these elements and, particularly, Pd, which reaches 230–240 ppb (Table 6). This difference is also evident from the primitive-mantle normalized [43] patterns of the PGEs (Figure 7). This supports the mineralogical evidence, and although bulk PGE analyses reported in this study are not enough for robust statistical implications, they are in agreement with the data of [28,42], which show the same noble metal systematics and additionally provide contents of Os, Ir and Rh.

Table 6. Bulk rock noble metal concentrations (ppb) in magnetite and amphibole clinopyroxenites. K4-30 and K4-20—our data; KK10 and KK12—from [42].

Sample	Type	Os	Ir	Ru	Rh	Pt	Pd	Au
K4-30	Amp Cpx-te	<10	<3	<5	<5	49	237	33
K4-20	Mag Cpx-te	<10	<3	<5	<5	17	19	19
KK10	Mag Cpx-te	0.7	0.1	-	1.2	1.5	7.4	4.5
KK12	Amp Cpx-te	0.3	0.1	-	0.3	38	157	8.5

5. Discussion

5.1. Comparison to Other Cu-Noble Metal Occurrences in the UA-Type Clinopyroxenites

Noble metal mineralization in clinopyroxenites of the Ural platinum belt is studied relatively poorly, insofar as copper–noble metal ores hosted by ultramafic rocks of the UPB have been studied in detail only for the Baronskoe deposit [29]. In this occurrence, noble metal minerals are represented by vysotskite PdS , kotulskite, stillwaterite Pd_8As_3 , a series of unnamed Pd-As-Te phases and Pd-rich electrum [29] (Table 4). However, these clinopyroxenites are genetically linked with the Volkovsky complex [30], which attribution to the UA-type is controversial [6,36]. On the contrary, Kachkanar intrusion has been considered as an upper part of a UA-type intrusion [6]. Moreover, some studies unite Kachkanar intrusion and the neighboring clinopyroxenite–dunite Veresovoborsky and

Svetloborsky intrusions into a large single UA-type complex [5,13]. Previously, Volchenko et al. [28] published a geochemical review of the rocks of the Kachkanar intrusion, particularly focusing on their noble metal potential. Although that study did not consider noble metal mineralogy in detail, it reported the presence of vysotskite (PdS), braggite (Pt,Pd)S with an admixture of Hg, aethenite, mertieite, kotulskite with an admixture of Hg, potarite, Pd-bearing tetraferroplatinum as well as alloys of Cu-Pd and Au-Ag-Pd compositions [28] (Table 4).

Similar styles of noble metal mineralization, tightly associated with copper sulfides, have been reported for several UA-type complexes of North America: Salt Chuck, Tulameen (Alaska) and Turnagain (British Columbia) [44–53].

In the Salt Chuck complex, PGM and copper ores (0.95% Cu, 19.9 g/t Au, 7 g/t Ag, and 26.1 g/t Pd on average) are hosted by biotite-bearing magnetite clinopyroxenite and gabbro with the richest zones being controlled by fault zones [44,48,52]. Noble metal minerals have been reported to be enclosed by sulfides, and dominated by kotulskite, often intergrown with hessite. Temagamite and isolated grains of Au-rich sperrylite and kotulskite are not uncommon for the Salt Chuck gabbros and pyroxenites as well [44].

In the Turnagain complex, clinopyroxenites and wehrlites host massive and semimassive Ni-Cu-Fe ores, which have been suggested to originate from silicate–sulfide immiscibility [44,45]. Furthermore, [46] reported disseminated (~5%) sulfide Cu-Fe ores with minor pyrite, pentlandite, arsenides, As-Sb sulfides and PGMs which include sperrylite (Pt₂As), sudburyite (Pd,Ni)Sb, Pd-rich melonite (Ni,Pd)Te₂, hongshiite PtCu, testibiopalladinite PdTe(Sb,Te) and genkinite (Pt₄Sb₃). These PGMs have been reported to occur mainly as small (<40 µm) inclusions hosted by sulfides of Cu, Fe, Ni and Co [46].

In the Tulameen complex, chalcopyrite–bornite–pyrite mineralization, containing PGMs, is hosted by magnetite–amphibole pyroxenites. Among the PGMs identified were sperrylite, isomertieite Pd₁₁Sb₂As₂ and some Pd-Te-Sb unnamed phases [47].

Copper–noble metal mineralization of the Kachkanar clinopyroxenites is most similar to the ones of Salt Chuck and Tulameen complexes. The sulfide-PGM assemblage of the Turnagain complex is somewhat different, being characterized by elevated Ni abundance in sulfides and PGMs. Therefore, Cu-Fe sulfide and noble metal assemblage of the Kachkanar intrusion clinopyroxenites are generally typical for the clinopyroxenites of the UA-type complexes, particularly to those of the economic Salt Chuck sulfide deposit and occurrences of the Tulameen complex.

5.2. Clinopyroxenite-, Dunite- and Gabbro- Hosted Noble Metal Assemblages

Comparison of the studied noble metal assemblage and that of dunites of the Svetloborsky and Veresovoborsky intrusions (parts of the same Kachkanar complex) as well as the other UPB dunites shows that the clinopyroxenitic and dunitic lithologies have generally contrasting sets of the PGMs. Platinum-group minerals from dunites and dunite-hosted chromitites are dominated by Pt-Fe intermetallides (largely primary isoferroplatinum) and minerals of the iridium-group PGEs (IPGEs): native osmium and iridium, laurite and erlichmanite. The secondary assemblage includes mainly tetraferroplatinum, tulameenite, ferronickelplatinum, cooperite, kashinite, ferrorhodsitite and various PGE thiospinels [4,11,12,14,15,17,18]. On the contrary, clinopyroxenites host mainly chalcogenides of Pd and Ag as well as electrum and Au native.

On the other hand, there is some overlap between dunitic and clinopyroxenitic noble metal assemblages. Firstly, secondary minerals for the dunitic PGMs set also include chalcogenides and Pd-Pb minerals, which may occupy up to 15 vol. % of the PGM nuggets: Pt arsenides and sulfoarsenides, potarite, zvyagentsevite Pd₃Pb, plumbopalladinite Pd₃Pb₂ and unnamed Pb-Te-Bi phases ([41] and unpublished authors' data). Secondly, late-stage sperrylite in the PGM assemblage of the Veresovoborsky intrusion contains up to 2.3–3 wt.% Pd [17,41]. Thirdly, the presence of Pd-bearing tetraferroplatinum has been previously reported in Kachkanar clinopyroxenites [27]. Finally, Pd-rich (up to 7–8 wt.% Pd) tulameenite [4], tetraferroplatinum [12] and Rh-Ir-Pt thiospinels [11] were found in chromitites

of the Uktus and Kytlym UA-type complexes of the UPB. These features superficially bridge dunitic and clinopyroxenitic noble metal assemblages, showing that they may rather represent different stages of a magmatic (fluid-magmatic) evolution than be completely unrelated to each other.

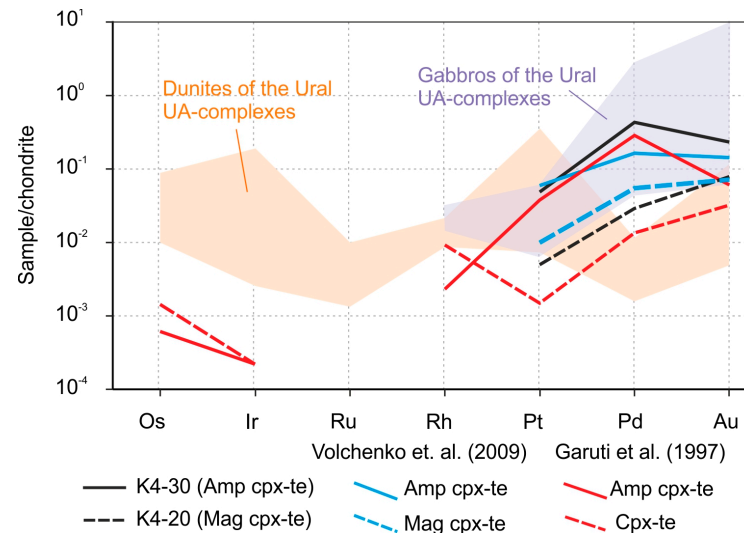


Figure 7. Chondrite-normalized [43] noble metal spider diagram for the magnetite and amphibole clinopyroxenites of the Kachkanar intrusion compared to the field of typical compositions of dunites and gabbros of the UPB UA-type complexes ([11] and references therein). Data are from this study and [28,42].

Furthermore, noble metal mineralization in the clinopyroxenites is similar to that in gabbroic rocks of the UA-type complexes. Although noble metal mineralogy of the Kachkanar complex gabbros has not been studied, a comparison of the studied mineral assemblages with those of the gabbros of the Serebryansky Kamen' [22] and Kumba [23] intrusions shows that both have Pd and Au specifics and are devoid of Pt and IPGE (Ir, Os, Ru) minerals (Figure 7). Moreover, in both clinopyroxenitic and gabbroic suites, noble metal mineralization associates with Cu-sulfides and occurs in amphibole-rich varieties. Although in the cases reported [22,23] the gabbro-hosted mineralization contains more Pd arsenides than the studied clinopyroxenites, it could be due to variations of the chalcogens' proportions in the parental magmas. We expect that similar studies of the PGE and PGM systematics of the Mt. Sarannaya gabbros (Figure 1) will shed more light on the PGM fractionation in the Kachkanar UA-type complex itself.

As the bottom line, bulk rock distribution of the noble metals in dunites and clinopyroxenites of the Kachkanar, Svetloborsky and Veresovoborsky intrusions reveals a strong fractionation of these metals: IPGEs and Pt concentrate in dunites, while Pd, Au and Ag—in clinopyroxenites [18]. Furthermore, the PGE patterns of the clinopyroxenites are more similar to the gabbroic ones (Figure 7). Such a distribution of the noble metals is reported characteristic of the other Ural–Alaskan-type complexes worldwide [50,54]. Therefore, our mineralogical and geochemical data on the noble metal mineralogy in clinopyroxenites of the Kachkanar intrusion are consistent with this “common UA-type pattern” and perfectly corroborate it.

5.3. Origin of the Mineralization

The formation of clinopyroxenites of the UA-type complexes and the Kachkanar intrusion particularly, remains debatable. It had been suggested that such rocks are formed due to either metasomatic transformation of dunitic rocks by basaltic melts [9,38] or some fluids [55]. Further studies advocated that clinopyroxenites of the UA-type complexes form from H₂O-saturated basaltic magmas at high oxygen fugacity (around the NNO buffer) and

temperatures of ca. 1100 °C [48] or some specific “wehrlitic” magmas [56]. Currently, the most acknowledged hypothesis proposes that these rocks primarily formed from high-Ca ankaramitic magmas as near-cotectic olivine–clinopyroxene (ideally ~10 and ~90 vol. %, respectively) cumulates, containing various amounts of a spinel phase (Cr-magnetite and magnetite) [4,25–27]. In this scenario, the formation of clinopyroxenites appears to be an intermediate stage of a high-Ca mafic/ultramafic melt differentiation, which regularly follows the crystallization of the early olivine–chromite cumulates (dunites).

During such a differentiation, the composition of spinel-group minerals, which crystallize along with the silicates, changes from chromite and Al-rich chromite to Cr-Ti magnetite as Cr is exhausted from the melt. The onset of abundant magnetite crystallization, which occurs generally during the olivine–clinopyroxene cotectic [54], results in a reduction of the melt, turns significant S^{4+} into S^{2-} form and may promote silicate–sulfide immiscibility [54]. Importantly, in this scenario, sulfides form after major olivine has been crystallized and thus should have high Cu/Ni ratios.

Finally, after a “protholith” of a UA-type complex, consisting of a dunite–clinopyroxenite–gabbro cumulate sequence, possibly with minor interstitial melts and fluids, is mostly formed, it is apparently subjected to tectonic deformation, which is evident from their largely “diapiric” occurrence and petrostructural data [5,57,58]. During this stage, fractured and permeable zones may control migration and concentration of late- and postmagmatic liquids (fractionated melts and fluids).

Within this petrological context, clinopyroxenite-hosted PGM-sulfide assemblages in the UA-type complexes have been considered as (1) crystallized from some “ore-bearing” fluids seeping mainly along the clinopyroxenite–gabbro boundaries [51,59] or (2) originated via solely silicate–sulfide immiscibility [45] or (3) formed during both magmatic and hydrothermal processes [29,44,48,60].

Our data distinctly show that the noble metal minerals associate with the sulfides and were apparently syngenetic with the latter. On the one hand, this could lead to a conclusion that the noble metals concentrated into a Cu-rich sulfide melt when the “magnetite-crisis”-related immiscibility occurred [48] and precipitated as chalcogenides at the terminal stages of sulfide liquid crystallization [61]. On the other hand, magnetite clinopyroxenites, which in this case should have been rich in sulfides and noble metals, contain relatively scarce mineralization and are poorer in the PGEs than the amphibole clinopyroxenites (Table 1, Figures 5 and 7). Therefore, we deem that the two-stage (magmatic + hydrothermal) model similar to that suggested by [48] could explain the features observed.

At the 1st stage, a small amount of base metal sulfide melt was generated due to the magnetite-related redox shift. This event formed disperse sulfides within magnetite clinopyroxenites (Figure 8A), which compose the majority of the Kachkanar clinopyroxenite body and host the studied mineralized dyke. The composition and proportions of these sulfides roughly corresponded to an “orthomagmatic” base metal assemblage with nearly equal amounts of pyrrhotite and chalcopyrite (Figure 5a), while pentlandite was deficient apparently due to a lack of Ni after olivine crystallization. Then, exsolution of H_2O -rich fluid from a magnetite + clinopyroxene(+olivine) cumulate pile resulted in a partial resorption of these sulfides [62,63] and enrichment of this fluid with S and other chalcophile elements, including noble metals (Figure 8B). At the same time, cumulate compaction, tectonic processes and, likely, diapirism of the near-solidus body, produced low-coherent and more permeable zones, which acted as pathways for the late-magmatic melts and fluids (Figure 8A).

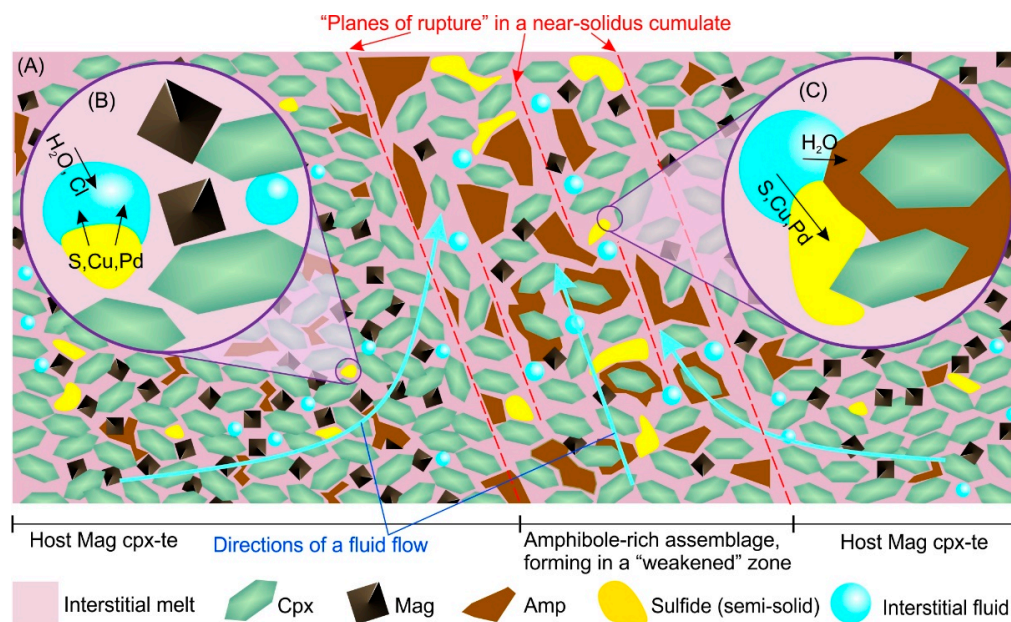


Figure 8. A schematic sketch of the fluid-assisted remobilization and concentration of the noble metals in Kachkanar clinopyroxenites (stage 2, see text for the details). (A) = a near-solidus cumulate with the planes of rupture and weakened zones forming due to compaction and deformation; (B) = cumulate degassing accompanied by dissolution of sulfides and scavenging of the chalcophile elements by fluids; (C) = a fluid–cumulate reaction and reprecipitation of sulfides and chalcophile elements in a “fluid conduit”.

At the 2nd stage, migration of these liquids through those pathways produced heterogeneous amphibolization of the clinopyroxenites and formed amphibole-rich “dykes”, one of which is considered here (Figure 8A). As H_2O from the fluid reacted with clinopyroxenes to form amphiboles, the concentration of S and chalcophile elements in the liquids increased, reaching saturation and, finally, formed Cu-rich sulfide mineralization within the amphibole clinopyroxenites (Figure 8C). Alternatively, pyrrhotite could have been initially formed but then was lost due to oxidation, as was proposed for the Platinoval reef of the Skaergaard intrusion [64]. Since the process of sulfide redeposition has been controlled by weakened zones, the resulting sulfide mineralization after this stage could have been strongly heterogeneous, even within the amphibole clinopyroxenites themselves.

Noteworthy, the 2nd-stage sulfide and noble metal concentration was apparently continuous and lasted until relatively low-temperature conditions. This is implied by (1) two generations of sulfide mineralization (bornite–chalcopyrite–magnetite and pyrite–chalcopyrite), (2) formation of the chlorite–actinolite edging of the chalcopyrite veins, characteristic of the second generation and (3) abundance of Te- and, particularly, Hg-rich mineral phases, that are typical for low-T epithermal conditions (e.g., [65]). The possibility of a continuous transport of Pd by fluids, rich in S and Cl, until relatively low-T conditions is supported by numerous empirical and theoretical studies (e.g., [66–68]).

5.4. Fractionation of the Noble Metals during Formation of the UA-Type Complexes

Although from examples of the Alaskan UA-type complexes it is well known that dunitic and chromititic lithologies are Pt- and IPGE-rich, while clinopyroxenites and gabbros concentrate Pd, Au, Cu and other chalcophile elements, there is a lack of petrological details which explain such a distribution. If it is assumed that the UA-type complexes are primarily formed due to fractional crystallization of a high-Mg, high-Ca (picritic or ankaramitic) melt within supra-subduction settings, then at the earliest stage chromite crystallizes along with olivine to form dunites. At relatively oxidized conditions, sulfide saturation is not reached, and the PGEs do not exhibit their chalcophile features. It has

been shown that in such circumstances, Os, Ir and Ru tend to be compatible with chromite, and, partially, olivine [69–71]. At the same time, direct crystallization of Os-, Ir-, Ru-, Rh- and Pt-bearing alloys and intermetallics takes place at the chromite-melt boundary zone, possibly due to a local reduction of the melt around chromite [72]. Notably, abundant micro- and nanoscale crystalline PGM inclusions are particularly characteristic for Cr-spinel from primitive volcanics [73]. These processes result in the melt's early-magmatic depletion in these metals, which is also largely manifested in geochemical patterns of the arc volcanics [74–80].

On the contrary, Pd, Au, Ag (and Cu) are relatively incompatible with both chromite and olivine and tend to accumulate in a melt during its differentiation [76]. Therefore, at the time when the magnetite begins to crystallize and the first sulfide fraction may form, the melt is already depleted in the IPGEs, Pt (and Ni, which partitioned into olivine), while enriched in Pd, Au, Ag (and Cu). The separating sulfide fraction inherits this systematics of the noble and chalcophile metals and concentrates them within magnetite clinopyroxenites [54]. Subsequent fluid processes may additionally fractionate the noble metals, concentrating more mobile elements such as Pd, Au, Ag, Hg and Te in amphibole-rich lithologies, and leaving Pt, Ni and, possibly, Cu in dispersed sulfide mineralization in the pristine magnetite clinopyroxenites.

Mineralogical (this study and [28]) and geochemical [18] data on the Kachkanar clinopyroxenites corroborate this theory, showing the strongly fractionated noble metal composition of these rocks (Figure 7). Furthermore, the fact that the dunites of the Veresovoborsky and Svetloborsky intrusions (as well as UPB dunites in general) are poor in Pd, Au and Ag minerals, while clinopyroxenites contain very few Pt minerals, implies that the formation of the PGE–chromite and PGE–sulfide assemblages were not temporary and spatially related. Likely, even if liquids that form chromite-hosted PGE mineralization reached sulfide saturation, they were Pd-deficient. On the contrary, sulfide melt, which formed a “protholith” for the sulfide–PGE mineralization, should have reacted with Pd–Au- and Ag-bearing evolved silicate melt and become enriched in these metals. At the same time, dunitic and clinopyroxenitic noble metal assemblages are not completely different and do share some common minerals (tetraferroplatinum, potarite and other Pd chalcogenides). This provides a link between these types of mineralization and suggests that they may represent different stages of the evolution of a single magmatic system, as predicted by [54].

6. Conclusions

Sulfide-rich amphibole clinopyroxenites, hosted by sulfide-poor magnetite clinopyroxenites of the Kachkanar intrusion, contain noble metal mineralization, with a composition similar to that in clinopyroxenites of the Alaskan UA-type complexes (Tulameen and Salt Chuck) [44–53]. The mineralization comprises palladium and silver tellurides (keithconnite Pd_{3-x}Te , sopcheite $\text{Ag}_4\text{Pd}_3\text{Te}_4$, stutzite $\text{Ag}_{5-x}\text{Te}_3$, hessite Ag_2Te and merenskyite PdTe), Pd bismotellurides (kotulskite $\text{Pd}(\text{Te},\text{Bi})$), Pd–Hg chalcogenides (temagamite Pd_3HgTe , atheneite $(\text{Pd},\text{Hg})_3\text{As}$), potarite PdHg , electrum AuAg and Hg-bearing native silver. Among those, six mineral phases have been first reported for clinopyroxenites of the UPB. Abundances of noble metals, sulfide minerals and amphibole are directly linked, suggesting the chalcophile behavior of the noble metals and a fluid-assisted origin of the mineralization. We suggest a two-stage model for the origin of the mineralization: (1) initial separation of a Cu-rich sulfide melt, enriched in Pd, Au, Ag and other chalcophile elements during crystallization of magnetite clinopyroxenites; (2) fluid-assisted redeposition of the sulfides and noble metals and their concentration in “dykes” of amphibole clinopyroxenites. Furthermore, as the Kachkanar intrusion is part of a large Kachkanar UA-type complex, which includes Svetloborsky and Veresovoborsky clinopyroxenite–dunite intrusions, these data, together with the PGE mineralogy of the dunites, make this complex a good record of the noble metal fractionation and highlight a contrasting behavior of IPGE + Pt and Pd + Ag + Au during the formation of the UA-type complexes. Finally, given that the gabbroic intrusion of Mt. Sarannaya, which is located northwards from the Kachkanar intrusion

(Figure 1), is attributed to this UA-type complex as well [37], it may be possible to use these four intrusions in a reconstruction of the “first crystals-to-deuteric alteration” behavior of the noble metals during fractionation of magmas, parental for the UA-type complexes.

Author Contributions: Conceptualization, S.Y.S., I.F.C. and R.S.P.; methodology, S.Y.S. and R.S.P.; investigation, S.Y.S., R.S.P. and A.V.K., writing—original draft preparation, S.Y.S. and I.F.C.; writing—review and editing, R.S.P.; visualization, R.S.P. and I.F.C.; supervision S.Y.S. All authors have read and agreed to the published version of the manuscript.

Funding: The research was supported by the Russian Science Foundation (project No. 22-17-00027).

Data Availability Statement: Data are contained within the article.

Acknowledgments: We thank our dear colleagues Vladimir Mikhailov and Nadezhda Vakhrusheva (R.I.P.) for their assistance in fieldwork and informal discussion of the results and implications.

Conflicts of Interest: The authors declare no conflict of interest.

References

1. Le Maitre, R.W.; Streckeisen, A.; Zanettin, B.; Le Bas, M.; Bonin, B.; Bateman, P. *Igneous Rocks: A Classification and Glossary of Terms: Recommendations of the International Union of Geological Sciences Subcommittee on the Systematics of Igneous Rocks*; Cambridge University Press: Cambridge, UK, 2005; p. 236.
2. Irvine, T.N. *Petrology of the Duke Island Ultramafic Complex Southeastern Alaska*; Geological Society of America: Boulder, CO, USA, 1974.
3. Presnall, D.; Dixon, S.A.; Dixon, J.R.; O'donnell, T.; Brenner, N.; Schrock, R.; Dycus, D. Liquidus phase relations on the join diopside-forsterite-anorthite from 1 atm to 20 kbar: Their bearing on the generation and crystallization of basaltic magma. *Contrib. Mineral. Petrol.* **1978**, *66*, 203–220. [\[CrossRef\]](#)
4. Pushkarev, E.V. *Petrology of the Uktus Dunite-Clinopyroxenite-Gabbro Massif (Middle Urals)*; Ural Branch of the Russian Academy of Sciences: Yekaterinburg, Russia, 2000; 296p. (In Russian)
5. Guillou-Frottier, L.; Burov, E.; Augé, T.; Gloaguen, E. Rheological conditions for emplacement of Ural–Alaskan-type ultramafic complexes. *Tectonophysics* **2014**, *631*, 130–145. [\[CrossRef\]](#)
6. Fershtater, G.B.; Bea, F.; Pushkarev, E.V.; Garuti, G.; Montero, P.; Zaccarini, F. Insight into the petrogenesis of the Urals Platinum Belt: New geochemical evidence. *Geochem. Int.* **1999**, *37*, 302–319.
7. Vysotskiy, N.K. Platinum deposits of the Isovsky and Nizhnii Tagil districts on the Urals. *Tr. Geo. Kom. Nov. Ser.* **1913**, *62*. (In Russian)
8. Duparc, L.; Tikhonovitch, M. *Le Platine et les Gites Platiniferes de l'Oural et du Monde*; Imprimerie et Lithographie: Geneve, Switzerland, 1920; 542p. (In French)
9. Zavaritsky, A.N. *Korennyye Mestorozhdeniya Platiny na Urale (Original Platinum Deposits on the Urals)*; Geological Committee: Leningrad, Russia, 1928. (In Russian)
10. Lazarenkov, V.G.; Malitch, K.N.; Sakhyanov, L.O. *Platinum Metal Mineralization of Zonal Ultrabasic and Comatiite Massifs*; Nedra: Leningrad, Russia, 1992; 217p. (In Russian)
11. Garuti, G.; Pushkarev, E.; Zaccarini, F. Composition and paragenesis of Pt-alloys from Ural-Alaskan type chromitites at Kitlim and Uktus (the Urals, Russia). *Can. Min.* **2002**, *40*, 1127–1146. [\[CrossRef\]](#)
12. Garuti, G.; Pushkarev, E.V.; Zaccarini, F.; Cabella, R.; Anikina, E.V. Chromite composition and platinum-group mineral assemblage in the Uktus Alaskan-type complex (Central Urals, Russia). *Min. Dep.* **2003**, *38*, 312–326. [\[CrossRef\]](#)
13. Auge, T.; Genna, A.; Legendre, O.; Ivanov, K.S.; Volchenko, Y.A. Primary platinum mineralization in the Nizhny Tagil and Kachkanar ultramafic complexes, Urals, Russia: A genetic model for PGE concentration in chromite-rich zones. *Econ. Geol.* **2005**, *100*, 707–732. [\[CrossRef\]](#)
14. Tolstykh, N.D.; Telegin, Y.M.; Kozlov, A.P. Platinum mineralization of the Svetloborsky and Kamenushinsky massifs (Urals Platinum Belt), Russ. *Geol. Geophys.* **2011**, *52*, 603–619. [\[CrossRef\]](#)
15. Tolstykh, N.; Kozlov, A.; Telegin, Y. Platinum mineralization of the Svetly Bor and nizhny tagil intrusions, Ural Platinum Belt. *Ore Geol. Rev.* **2015**, *67*, 234–243. [\[CrossRef\]](#)
16. Stepanov, S.Y.; Palamarchuk, R.S.; Khanin, D.A.; Varlamov, D.A.; Antonov, A.V. The Distribution and Speciation of PGEs in Chromitite from the Svetloborsky, Veresovoborsky, and Kamenushensky Clinopyroxenite–Dunite Massifs (Middle Urals). *Mosc. Univ. Geol. Bull.* **2018**, *73*, 527–537. [\[CrossRef\]](#)
17. Stepanov, S.; Antonov, A.; Palamarchuk, R.; Varlamov, D.; Khanin, D.; Kozlov, A. Morphology, composition, and ontogenesis of platinum-group minerals in chromitites of zoned clinopyroxenite-dunite massifs The Middle Urals. *Russ. Geol. Geophys.* **2020**, *61*, 41–67. [\[CrossRef\]](#)
18. Stepanov, S.Y.; Palamarchuk, R.S.; Kutyrev, A.V.; Shilovskikh, V.V.; Petrov, S.V. Mineralogy and geochemistry of platinum-group elements in the zoned mafic-ultramafic intrusions of the Uralian Platinum belt, Russia. *J. Geochem. Explor.* **2023**, *246*, 107155. [\[CrossRef\]](#)

19. Poltavets, Y.A.; Poltavets, Z.I.; Nechkin, G.S. Volkovsky deposit of titanomagnetite and copper-titanomagnetite ores with accompanying noble-metal mineralization, the Central Urals, Russia. *Geol. Ore Depos.* **2011**, *53*, 126–139. [[CrossRef](#)]
20. Anikina, E.V.; Malitch, K.N.; Pushkarev, E.V.; Shmelev, V.R. The Nizhny Tagil and Volkovsky massifs of the Uralian Platinum Belt, and related deposits. In *Field Trip Guidebook, Proceedings of the 12th International Platinum Symposium, Yekaterinburg, Russia, 11–14 August 2014*; IGG UB RAS: Yekaterinburg, Russia, 2014.
21. Murzin, V.V.; Palyanova, G.A.; Anikina, E.V.; Moloshag, V.P. Mineralogy of noble metals (Au, Ag, Pd, Pt) in Volkovskoe Cu-Fe-Ti-V deposit (Middle Urals, Russia). *LITHOSPHERE* **2021**, *21*, 653–659. (In Russian) [[CrossRef](#)]
22. Mikhailov, V.V.; Stepanov, S.Y.; Kozlov, A.V.; Palamarchuk, R.S.; Shilovskikh, V.V.; Abramova, V.D. New Copper–Precious Metal Occurrence in Gabbro of the Serebryansky Kamen Massif, Ural Platinum Belt, Northern Urals. *Geol. Ore Depos.* **2021**, *63*, 528–555. [[CrossRef](#)]
23. Mikhailov, V.V.; Stepanov, S.Y.; Petrov, S.V.; Palamarchuk, R.S. Precious metal mineralization in gabbroids of the Kumba intrusive, the Uralian platinum belt (North Urals). *Mineralogy* **2022**, *8*, 79–93. (In Russian) [[CrossRef](#)]
24. Irvine, T.N. Bridget Cove volcanics, Juneau area, Alaska: Possible parental magma of Alaskan-type ultramafic complexes. *Carnegie Inst. Yearb.* **1973**, *72*, 1972–1973.
25. Batanova, V.G.; Pertsev, A.N.; Kamenetsky, V.S.; Ariskin, A.A.; Mochalov, A.G.; Sobolev, A.V. Crustal evolution of island-arc ultramafic magma: Galmoenan pyroxenite–dunite plutonic complex, Koryak Highland (Far East Russia). *J. Petr.* **2005**, *46*, 1345–1366. [[CrossRef](#)]
26. Pushkarev, E.V.; Kamenetsky, V.; Gottman, I.; Yaxley, G. The PGM-bearing volcanic ankaramite (Urals, Russia): Bridging ankaramite parental magmas and the Ural-Alaskan-type intrusions. In *Proceedings of the 12th International Platinum Symposium, Yekaterinburg, Russia, 11–14 August 2014*; Institute of Geology and Geochemistry UB RAS: Yekaterinburg, Russia, 2014; pp. 204–205.
27. Chayka, I.F.; Baykov, N.I.; Kamenetsky, V.S.; Kutyrev, A.V.; Pushkarev, E.V.; Abersteiner, A.; Shcherbakov, V.D. Volcano–Plutonic Complex of the Tumrok Range (Eastern Kamchatka): An Example of the Ural-Alaskan Type Intrusion and Related Volcanic Series. *Minerals* **2023**, *13*, 126. [[CrossRef](#)]
28. Volchenko, Y.A.; Koroteev, V.A.; Nesterova, S.I. Comparative characteristics of platinum-bearing ferroclinopyroxenite complexes of the Ural mobile belt. In *Yearbook-2008 of IGG UrO RAS*; Institute of Geology and Geochemistry UB RAS: Ekaterinburg, Russia, 2009; pp. 209–216. (In Russian)
29. Zaccarini, F.; Anikina, E.; Pusharev, E.; Rusin, I.; Garuti, G. Palladium and gold minerals from the Baronskoe-Kluevsky ore deposit (Volkovsky complex, Central Urals, Russia). *Min. Pet.* **2004**, *82*, 137–156. [[CrossRef](#)]
30. Anikina, E.V.; Alekseev, A.V. Mineralogical and geochemical characteristics of gold-palladium mineralization in the Volkovsky gabbro-diorite massif (Platinum-bearing belt of the Urals). *Lithosphere* **2010**, *5*, 75–100. (In Russian)
31. Herrington, R.J.; Zaykov, V.V.; Maslennikov, V.V.; Brown, D.; Puchkov, V.N. Mineral deposits of the Urals and links to geodynamic evolution. *Econ. Geol.* **2005**. [[CrossRef](#)]
32. Stepanov, S.Y.; Pilyugin, A.G.; Zolotarev, A.A., Jr. Comparison of the compositions of the platinum group minerals of the chromitites and placers of the Nizhny Tagil massif, Middle Urals. *J. Min. Inst.* **2015**, *211*, 22–28. (In Russian)
33. Stepanov, S.Y.; Palamarchuk, R.S.; Kozlov, A.V.; Khanin, D.A.; Varlamov, D.A.; Kiseleva, D.V. Platinum-group minerals of Pt-placer deposits associated with the Svetloborsky Ural-Alaskan type massif, Middle Urals, Russia. *Minerals* **2019**, *9*, 77. [[CrossRef](#)]
34. Ivanov, K.S.; Shmelev, V.R. Platiniferous belt of the Urals—A magmatic trace of early Palaeozoic subduction zone. *Rep. Russ. Acad. Sci.* **1996**, *347*, 649–652. (In Russian)
35. Ivanov, K.S.; Vinnichuk, N.N.; Volchenko, Y.A.; Yerokhin, Y.V.; Augé, T.; Genna, A. The platiniferous Urals belt nature: New geological-geophysical data. *Tecton. Geophys. Lithosphere* **2002**, *1*, 213–216. (In Russian)
36. Fershtater, G.B. The main features of the Uralian Paleozoic magmatism and the epiocceanic nature of the orogen. *Min. Pet.* **2013**, *107*, 39–52. [[CrossRef](#)]
37. Desyatnichenko, L.I.; Fadeicheva, I.F.; Parfenov, V.V. (Eds.) *State Geological Map of the Russian Federation, Scale 1:200,000*, 2nd ed.; The Sredneural'skaya Series; Sheet O-40-XII (Kachkanar): Explanatory Note; VSEGEI: St. Petersburg, Russia, 2005; 457p.
38. Fominykh, V.G.; Samoilov, P.I.; Maksimov, G.S.; Makarov, V.A. *Pyroxenites of Kachkanar*; UFAN USSR: Sverdlovsk, Russia, 1967; 84p. (In Russian)
39. Puchkov, V.N. Structural stages and evolution of the Urals. *Min. Pet.* **2013**, *107*, 3–37. [[CrossRef](#)]
40. Warr, L.N. IMA-CNMNC approved mineral symbols. *Min. Mag.* **2021**, *85*, 291–320. [[CrossRef](#)]
41. Stepanov, S.Y.; Palamarchuk, R.S.; Varlamov, D.A.; Kozlov, A.V.; Khanin, D.A.; Antonov, A.V. Platinum Group Minerals from Veresovka River Deluvial Placer, Veresovoborsky Dunite–Clinopyroxenite Massif (Middle Urals). *Geol. Ore Depos.* **2019**, *61*, 767–781. [[CrossRef](#)]
42. Garuti, G.; Fershtater, G.; Bea, F.; Montero, P.; Pushkarev, E.; Zaccarini, F. Platinum-group elements as petrological indicators in mafic-ultramafic complexes of the central and southern Urals: Preliminary results. *Tectonophysics* **1997**, *27*, 181–194. [[CrossRef](#)]
43. McDonough, W.F.; Sun, S.-S. The composition of the Earth. *Chem. Geol.* **1995**, *120*, 223–253. [[CrossRef](#)]
44. Watkinson, D.H.; Melling, D.R. Genesis of Pd–Pt–Au–Ag–Hg minerals in Cu-rich sulfides; Salt Chuck mafic–ultramafic rock complex, Alaska. *Geol. Assoc. Can. Mineral. Assoc. Can. Program Abstr.* **1989**, *14*, A48.
45. Nixon, G.T. Ni–Cu sulfide mineralization in the Turnagain Alaskan-type complex: A unique magmatic environment. In *Geological Fieldwork*; BC Geol Surv Paper 1998–1; British Columbia Min Energy Mines: Victoria, BC, Canada, 1997.

46. Jackson-Brown, S.; Scoates, J.S.; Nixon, G.T.; Ames, D.E. Mineralogy of sulphide, arsenide, and platinum group minerals from the DJ/DB Zone of the Turnagain Alaskan-type ultramafic intrusion, north-central British Columbia. In *Geological Fieldwork 2013*; British Columbia Geol Surv Paper 2014–1; British Columbia Ministry of Energy and Mines: Victoria, BC, Canada, 2014.
47. Nixon, G.T.; Manor, M.J.; Scoates, J.S. Cu-PGE-sulphide mineralization in the Tulameen Alaskan type complex: Analogue for Cu-PGE reefs in layered complexes. *Br. Columbia Geol. Surv. Geofile* **2018**, *2*.
48. Loney, R.A.; Himmelberg, G.R. Petrogenesis of the Pd-rich intrusion at Salt Chuck, Prince of Wales Island: An early Paleozoic Alaskan-type ultramafic body. *Can. Miner.* **1992**, *30*, 1005–1022.
49. Thakurta, J.; Ripley, E.M.; Li, C. Platinum Group Element Geochemistry of Sulfide-Rich Horizons in the Ural-Alaskan-Type Ultramafic Complex of Duke Island, Southeastern Alaska. *Econ. Geol.* **2014**, *109*, 643–659. [[CrossRef](#)]
50. O'Driscoll, B.; González-Jiménez, J.M. Petrogenesis of the Platinum-Group Minerals. *Rev. Mineral. Geochem.* **2016**, *81*, 489–578. [[CrossRef](#)]
51. Gault, H.R. *The Salt Chuck Copper–Palladium Mine, Prince of Wales Island, Southeastern Alaska*; US Geological Survey, Open-File Rep. 4G19; US Department of The Interior: Washington, DC, USA, 1945.
52. Holt, S.P.; Shepard, J.G.; Thorne, R.L.; Tolonen, A.W.; Fosse, E.L. *Investigation of the Salt Chuck copper mine, Kasaan Peninsula, Prince of Wales Island, southeastern Alaska*; US Department of the Interior, Bureau of Mines: Washington, DC, USA, 1948; Volume 4358.
53. Clark, T. Geology of an Ultramafic Complex on the Turnagain River, Northwestern B.C. Ph.D. Thesis, Queens University, Kingston, ON, Canada, 1975. Unpublished.
54. Milidragovic, D.; Nixon, G.T.; Scoates, J.S.; Nott, J.A.; Spence, D.W. Redox-controlled chalcophile element geochemistry of the Polaris Alaskan-type mafic-ultramafic complex, British Columbia, Canada. *Can. Min.* **2021**, *59*, 1627–1661. [[CrossRef](#)]
55. Efimov, A.A. *Gabbro–Hyperbasite Complexes of the Urals and the Problems of Ophiolites*; Nauka: Moscow, Russia, 1984; 232p. (In Russian)
56. Popov, V.S.; Nikiforova, N.F. Ultramafic Rocks, Gabbroids, and Titanomagnetite Ore at Kachkanar, the Central Urals: An Integrated Petrological Model. *Geochemistry* **2004**, *1*, 11–25.
57. Bether, O.V. Petrology of Ultramafic Rocks of the Inagli Massif (Aldan Shield). Ph.D. Thesis, Tomsk State University, Tomsk, Russia, 1997; 21p. (In Russian).
58. Bodinier, J.-L.; Boudier, F.; Dautria, J.-M.; Bedini, R.M.; Burg, J.-P.; Pupier, E.; Balanec, J.-L.; Efimov, A.; Prikhodko, V.S. The Konder «Anorogenic» Ultramafic Massif (Aldan Shield): Impact of a translithospheric mantle diapir at the earth's surface? In Proceedings of the Fourth International Workshop on Orogenic Lherzolite and Mantle Processes, Samani, Hokkaido, Japan, 26 August–3 September 2002.
59. Mertie, J.B., Jr. Economic Geology of the Platinum Group metal. *USGS* **1969**, *630*, 119.
60. Helmy, H.M. Cu–Ni–PGE mineralization in the Genina Gharbia mafic–ultramafic intrusion, Eastern Desert, Egypt. *Can. Miner.* **2004**, *42*, 351–370. [[CrossRef](#)]
61. Mansur Eduardo, T.; Barnes, S.J.; Duran, C.J.; Sluzhenikin, S.F. Distribution of chalcophile and platinum-group elements among pyrrhotite, pentlandite, chalcopyrite and cubanite from the Noril'sk-Talnakh ores: Implications for the formation of platinum-group minerals. *Min. Dep.* **2020**, *55*, 1215–1232. [[CrossRef](#)]
62. Boudreau, A.E.; McCallum, I.S. Concentration of platinum-group elements by magmatic fluids in layered intrusions. *Econ. Geol.* **1992**, *87*, 1830–1848. [[CrossRef](#)]
63. Boudreau, A.E.; Meurer, W.P. Chromatographic separation of the platinum-group elements, gold, base metals and sulfur during degassing of a compacting and solidifying igneous crystal pile. *Contrib. Min. Pet.* **1999**, *134*, 174–185. [[CrossRef](#)]
64. Andersen, J.C. Postmagmatic sulphur loss in the Skaergaard intrusion: Implications for the formation of the Platinova Reef. *Lithos* **2006**, *92*, 198–221. [[CrossRef](#)]
65. Baksheev, I.A.; Vlasov, E.A.; Nikolaev, Y.N.; Krivitskaya, N.N.; Koshlyakova, N.N.; Nagornaya, E.V.; Kara, T.V.; Dzhezheya, G.T. Mineralogy of the Tumanny Au-Ag-Te-Hg epithermal veins, Western Chukchi Peninsula, Russia. *Ore Geol. Rev* **2018**, *101*, 293–311. [[CrossRef](#)]
66. Oberthür, T.; Melcher, F.; Fusswinkel, T.; van den Kerkhof, A.M.; Sosa, G.M. The hydrothermal Waterberg platinum deposit, Mookgophong (Naboomspruit), South Africa. Part 1: Geochemistry and ore mineralogy. *Min. Mag.* **2018**, *82*, 725–749. [[CrossRef](#)]
67. Sullivan, N.A.; Zajacz, Z.; Brenan, J.M.; Tsay, A. The solubility of platinum in magmatic brines: Insights into the mobility of PGE in ore-forming environments. *Geochim. Cosmochim. Acta* **2022**, *316*, 253–272. [[CrossRef](#)]
68. Tagirov, B.R.; Baranova, N.N.; Zotov, A.V.; Akinfiev, N.N.; Polotnyanko, N.A.; Shikina, N.D.; Koroleva, L.A.; Shvarov, Y.V.; Bastrakov, E.N. The speciation and transport of palladium in hydrothermal fluids: Experimental modeling and thermodynamic constraints. *Geochim. Cosmochim. Acta* **2013**, *117*, 348–373. [[CrossRef](#)]
69. Park, J.W.; Kamenetsky, V.; Campbell, I.; Park, G.; Hanski, E.; Pushkarev, E. Empirical constraints on partitioning of platinum group elements between Cr-spinel and primitive terrestrial magmas. *Geochim. Cosmochim. Acta* **2017**, *216*, 393–416. [[CrossRef](#)]
70. Brenan, J.M.; McDonough, W.F.; Ash, R. An experimental study of the solubility and partitioning of iridium, osmium and gold between olivine and silicate melt. *Earth Planet. Sci. Lett.* **2005**, *237*, 855–872. [[CrossRef](#)]
71. Brenan, J.M.; Finnigan, C.F.; McDonough, W.F.; Homolova, V. Experimental constraints on the partitioning of Ru, Rh, Ir, Pt and Pd between chromite and silicate melt: The importance of ferric iron. *Chem. Geol.* **2012**, *302*, 16–32. [[CrossRef](#)]
72. Finnigan, C.S.; Brenan, J.M.; Mungall, J.E.; McDonough, W.F. Experiments and models bearing on the role of chromite as a collector of platinum group minerals by local reduction. *J. Pet.* **2008**, *49*, 1647–1665. [[CrossRef](#)]

73. Kamenetsky, V.S.; Park, J.W.; Mungall, J.E.; Pushkarev, E.V.; Ivanov, A.V.; Kamenetsky, M.B.; Yaxley, G.M. Crystallization of platinum-group minerals from silicate melts: Evidence from Cr-spinel-hosted inclusions in volcanic rocks. *Geology* **2015**, *43*, 903–906. [[CrossRef](#)]
74. Dale, C.W.; Macpherson, C.G.; Pearson, D.G.; Hammond, S.J.; Arculus, R.J. Inter-element fractionation of highly siderophile elements in the Tonga Arc due to flux melting of a depleted source. *Geochim. Cosmochim. Acta* **2012**, *89*, 202–225. [[CrossRef](#)]
75. Park, J.-W.; Campbell, I.H.; Eggins, S.M. Enrichment of Rh, Ru, Ir and Os in Cr spinels from oxidized magmas: Evidence from the Ambae volcano, Vanuatu. *Geochim. Cosmochim. Acta* **2012**, *78*, 28–50. [[CrossRef](#)]
76. Park, J.W.; Campbell, I.H.; Kim, J.; Moon, J.W. The role of late sulfide saturation in the formation of a Cu- and Au-rich magma: Insights from the platinum group element geochemistry of Niuatahi-Motutahi lavas, Tonga rear arc. *J. Pet.* **2015**, *56*, 59–81. [[CrossRef](#)]
77. Kuttyrev, A.V.; Kamenetsky, V.S.; Park, J.; Maas, R.; Demonerova, E.I.; Antsiferova, T.N.; Ivanov, A.V.; Hwang, J.; Abersteiner, A.; Ozerov, A.Y. Primitive high-K intraoceanic arc magmas of Eastern Kamchatka: Implications for Paleo-Pacific tectonics and magmatism in the Cretaceous. *Pacific-Asian Tecton.* **2021**, *220*, 103703. [[CrossRef](#)]
78. Kuttyrev, A.V.; Zelenski, M.; Nekrylov, N.; Savelyev, D.; Kontonikas-Charos, A.; Kamenetsky, V.S. Noble metals in arc basaltic magmas worldwide: A case study of modern and pre-historic lavas of the Tolbachik volcano. *Front. Earth Sci.* **2021**, *9*, 791465. [[CrossRef](#)]
79. Savelyev, D.P.; Kamenetsky, V.S.; Danyushevsky, L.V.; Botcharnikov, R.E.; Kamenetsky, M.B.; Park, J.-W.; Portnyagin, M.V.; Olin, P.; Krashennnikov, S.P.; Hauff, F.; et al. Immiscible sulfide melts in primitive oceanic magmas: Evidence and implications from picrite lavas (Eastern Kamchatka, Russia). *Am. Mineral.* **2018**, *103*, 886–898. [[CrossRef](#)]
80. Savelyev, D.P.; Palesskii, S.V.; Portnyagin, M.V. The source of platinum group elements in basalts of the ophiolite complex of the Kamchatsky Mys Peninsula (Eastern Kamchatka). *Russ. Geol. Geophys* **2018**, *59*, 1592–1602. [[CrossRef](#)]

Disclaimer/Publisher’s Note: The statements, opinions and data contained in all publications are solely those of the individual author(s) and contributor(s) and not of MDPI and/or the editor(s). MDPI and/or the editor(s) disclaim responsibility for any injury to people or property resulting from any ideas, methods, instructions or products referred to in the content.